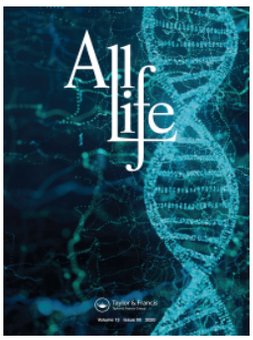

All Life

ISSN: (Print) (Online) Journal homepage: https://www.tandfonline.com/loi/tfls21

Development of synthetic thrombus models to simulate stroke treatment in a physical neurointerventional training model

Nadine Wortmann, Thomas Andersek, Helena Guerreiro, Anna A. Kyselyova, Andreas M. Frölich, Jens Fiehler & Dieter Krause

To cite this article: Nadine Wortmann, Thomas Andersek, Helena Guerreiro, Anna A. Kyselyova, Andreas M. Frölich, Jens Fiehler & Dieter Krause (2022) Development of synthetic thrombus models to simulate stroke treatment in a physical neurointerventional training model, All Life, 15:1, 283-301, DOI: 10.1080/26895293.2022.2046181

To link to this article: https://doi.org/10.1080/26895293.2022.2046181

Published online: 04 Mar 2022.

ALL LIFE
2022, VOL. 15, NO. 1, 283–301
https://doi.org/10.1080/26895293.2022.2046181

Taylor & Francis
Taylor & Francis Group

Development of synthetic thrombus models to simulate stroke treatment in a physical neurointerventional training model

Nadine Wortmann [a], Thomas Andersek[b], Helena Guerreiro [c], Anna A. Kyselyova [c], Andreas M. Frölich [d], Jens Fiehler [c] and Dieter Krause [a]

[a]Institute of Product Development and Mechanical Engineering Design, Hamburg University of Technology, Hamburg, Germany; [b]WEINMANN Emergency Medical Technology GmbH + Co. KG, Hamburg, Germany; [c]Department of Diagnostic and Interventional Neuroradiology, University Medical Center Hamburg-Eppendorf, Hamburg, Germany; [d]Röntgenpraxis im Tesdorpfhaus, Lübeck, Germany

ABSTRACT

In an ischaemic stroke, a blood clot (thrombus) occludes one of the arteries supplying the brain with oxygen. In such cases, a prompt and safe removal of the thrombus by interventional physicians is of high importance. The procedure of mechanical thrombectomy is mainly trained on animal models or simple flow models with animal- or human-based thrombi. The aim of this study is to develop a completely blood free thrombus model for use in an existing physical neurointerventional simulation model. Based on requirements established with treating physicians and supplemented by a broad literature review, a systematic material selection based on mechanical properties was performed by means of a material database. Selected materials, as well as other materials from a literature search and structural additive manufactured clots, were produced and selectively narrowed down, by means of functional property testing. Based on a pre-selection by a simple test set-up, the main tests were carried out on the existing simulation model by interventional physicians under realistic test conditions in a clinical angiography suite. As a result, four different types of thrombi varying in elasticity, solidity and fragmentation, were obtained by material combinations based on agarose and silicone in different concentrations and with further additives.

ARTICLE HISTORY
Received 28 September 2021
Accepted 2 February 2022

KEYWORDS
Synthetic thrombus; mechanical properties; systematic material selection; thrombectomy; physical simulation model; additive manufacturing

Introduction

Ischaemic stroke is one of the leading causes of disability and one of the most frequent causes of death in industrialized countries (Berkefeld 2018). It is mainly caused by an occlusion of the cerebral vessels by a blood clot, a so-called thrombus (Kreusch 2013). Since 1.9 million nerve cells are irreversibly destroyed within every minute of brain ischaemia (Saver 2006), rapid reopening of the affected vessel is of high priority. Thrombi are primarily dissolved with the procedure of thrombolysis. However, this procedure reaches its limits for thrombi above a certain size (more than 8 mm) and after a certain period of time (more than 6 h) (Gizewski 2014; Berkefeld 2018). Another procedure is the mechanical, invasive extraction of the thrombus by means of a stent retriever or aspiration. Combination of both intravenous thrombolysis and mechanical recanalization (thrombectomy) has proven to be successful and has become a gold standard in stroke treatment (Berkhemer et al. 2015; Goyal et al. 2015; Jovin et al. 2015; Saver et al. 2015).

Due to the increased use of thrombectomy as well as the difficult parameters, such as enormous time pressure and a wide range of different thrombi, training of the procedure by the treating physicians is of immense importance (Gizewski 2014; Paramasivam et al. 2014). Animal models are increasingly controversial for economic and ethical reasons (Wetzel et al. 2005; Paramasivam et al. 2014). Moreover they significantly differ from humans in their anatomy as well as in haemodynamic (Gralla et al. 2006). Thus, simple flow models or even more complex physical simulation models are increasingly used. However, these often use artificially generated animal blood thrombi (Chueh et al. 2012; Mokin et al. 2015). Exemplary Simon et al. (2014) describe the use of a synthetic thrombus made of polyurethane from the company Concentric Medical (Mountain View, California, USA). Yet, according to

CONTACT Nadine Wortmann nadine.wortmann@tuhh.de Institute of Product Development and Mechanical Engineering Design, Hamburg University of Technology, Denickestr. 17, Hamburg 21073, Germany

their own product information, these fail to accurately reproduce the diversity of human thrombi (Simon et al. 2014).

The aim of this study is to expand the Hamburg Anatomical Neurointerventional Simulator (HANNES) (cf. Chapter *Materials and method)* to include synthetic, animal ingredient-free thrombus models, by means of which realistic thrombectomy may be simulated. So far, a children's toy slime (Puupsie Slime, Simba-Toys GmbH & Co. KG, Fürth, Germany) has been used in the model for training courses for radiographers to create a vessel occlusion. In these courses, the focus is on the thrombectomy procedure itself as well as the assistant's function, while the behaviour of the thrombus is not the focus. In the training of the treatment procedure by physicians, clot behaviour plays a decisive role. The subject of this study is the development, production and testing of various thrombus models whose haptic properties in the model are similar to those in the human body. For this purpose, a systematic material selection is carried out on the basis of the requirements determined for the thrombus models and the mechanical properties of thrombi described in the literature, in order to determine potential materials. The material selection is further narrowed down in preliminary tests. The materials shown to be suitable will be assessed on HANNES by interventional neuroradiologists and compared to whole pig blood thrombi. Based on this assessment, further optimizations of the thrombus models will be carried. These will be repeatedly tested and assessed on HANNES (Guerreiro et al. 2021). Finally, four thrombus models are selected that represent different human thrombi in their haptic properties.

Fundamentals

Mechanical thrombectomy is an invasive procedure in which access is first gained to the arterial vascular system by puncturing the femoral or radial artery. Using different sized catheters and wires in a telescopic manner a microcatheter-microwire system is advanced to the occlusion site in the cerebral artery and then through the thrombus. In the next step, the microwire is removed from the microcatheter and the stent retriever is advanced through the microcatheter to the thrombus. Once the stent retriever is placed distally from the thrombus, it is released by pulling back the microcatheter. A wire mesh unfolds to integrate into the thrombus, thereby securing it to the stent retriever. Usually, a balloon attached to the head of the guide catheter, placed in the cervical artery, and inflated with an iodinated contrast solution so it is visible. The inflated balloon prevents blood flow towards the thrombus. Further negative pressure may be created by means of aspiration, through an intermediate catheter, with the aim of increasing retrograde blood flow and draw potential thrombus fragments into the guide catheter. Ideally, the thrombus is removed from the vessel by withdrawing the stent retriever into the intermediate or guide catheter under negative pressure. The catheter sequence is shown in Figure 1. The intervention is performed under digital subtraction angiography (DSA). In this procedure iodine-containing contrast medium is injected into the arteries through the catheter system, which leads to an X-ray image of the vasculature (Berkefeld et al. 2005; Ringleb et al. 2016; Lamprecht 2018; Weafer et al. 2019).

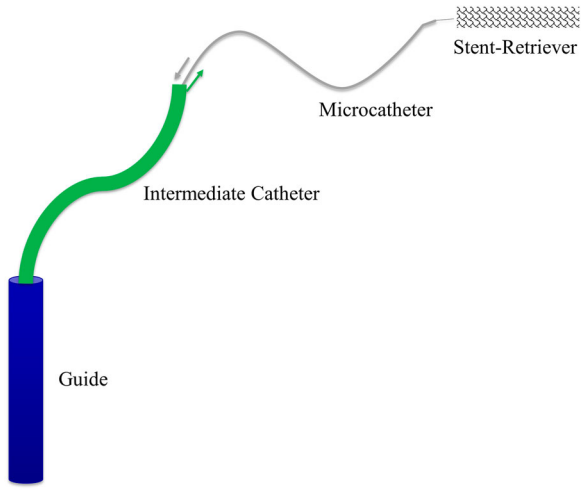

Figure 1. Schematic representation of the catheter sequence with guide, intermediate catheter, microcatheter and stent retriever.

In addition to the intervention itself, therapeutical success also depends on the type of thrombus. It has been shown that the characteristics of thrombi depend on their origin. According to Johnson et al. (Johnson et al. 2017) a thrombus is a solid mass composed of a network of fibrin, platelets and other blood components. Thrombi form as a result of the body's own clotting cascade due to an injury to a blood vessel or a significant reduction in blood flow (called stasis). They can be released into the bloodstream and lead to an

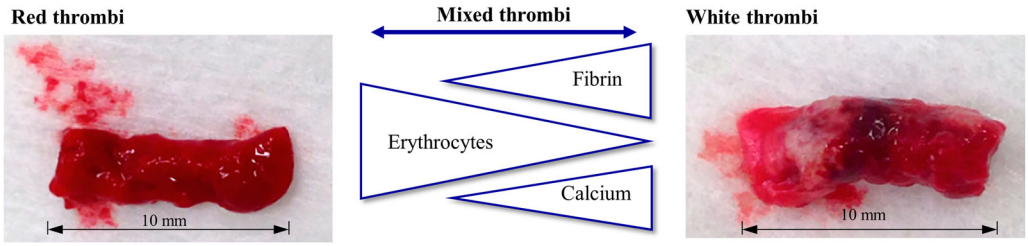

Figure 2. Thrombus types and their compositions. From red to white thrombi with increasing or decreasing amounts of fibrin, erythrocytes and calcium.

occlusion of another vessel, resulting in a disruption of the oxygen supply and causing an infarction. Depending on the trigger (micro-injury vs. stasis), thrombi with different compositions are formed.

In the case of micro-injury, deposition thrombi are formed. Thrombocytes attach themselves to the damaged vessel wall and are held together by a dense fibrin fibre network. Red erythrocytes are not completely enmeshed in this network and thus, this type of thrombus present with predominantly high proportions of platelets and fibrin. This leads to a white colouring of the thrombi, so that they are also known as 'white thrombi' (Lamprecht 2018; Müller-Esterl 2018; Staessens et al. 2020).

Large artery atherosclerotic and cryptogenic thrombi tend to have a higher percentage of erythrocytes (Maekawa et al. 2018; Liao et al. 2020), although recent publications imply that this is not always the case (Brinjikji et al. 2021). These thrombi with a high erythrocyte content are also referred to as 'red thrombi' (Lamprecht 2018; Müller-Esterl 2018).

In deposition thrombi, calcium may become embedded in the area of arteriosclerotic deposits, making the thrombus much firmer and stiffer (Wang et al. 2001; Chueh et al. 2012; Johnson et al. 2017). Mixed forms can also develop due to the occurrence of slowed blood flow as a result of a deposition thrombus. In this case, a thrombus forms with a light-coloured 'head' and a dark 'tail' (Lamprecht 2018).

Recently neutrophil extracellular traps (NETs) have been shown to be a factor in thrombus formation and composition, potentially having an influence on thrombus retrievability (Martinod and Wagner 2014).

Different types of thrombi and their main components, which influence their haptic behaviour are shown in Figure 2. Thrombi exhibit different mechanical properties according to their various compositions.

Wang et al. (2001) generally describe the behaviour of thrombi as incompressible, nonlinearly elastic, and heterogeneous. Johnson et al. (2017) show that the mechanical properties of thrombi resemble viscoelastic polymers with viscous and elastic properties. The literature described below describes the mechanical quantities of stress–strain relationship, elastic modulus, friction between thrombus and vessel wall, storage and loss modulus, density, and fragmentation. However, thrombi of different origin and composition as well as partly human and partly animal thrombi of different species were considered, so that the results cannot be applied to every type of thrombus. However, general trends about the factors influencing the mechanical properties of thrombi can be deduced (see Figure 4).

Chueh et al. (2011), Krasokha et al. (2010), Teng et al. (2015), Saldívar et al. (2002), and Ashton et al. (2009) investigated the stress–strain relationship. From these studies, the stress–strain relationship of thrombi changes from a linear to a non-linear behaviour at 70–100% strain. The strain limit of thrombi can take a value up to 300% and the tensile stress can be up to 10 kPa.

Boodt et al. were able to show that the stiffness of thrombectomised thrombi correlates with the thrombocyte and fibrin content (Boodt et al. 2021). The Young's modulus describes the ability of a material to withstand elastic deformation (Cardarelli 2008). Thus, a higher Young's modulus represents more stiffness, while a lower value represents elastic behaviour. In a qualitative test, Johnson et al. (2017) show that the Young's modulus of thrombi increases linearly with increasing fibrin content. Using ex vivo force-displacement measurements in rat thrombi of different ages, Xie et al. (2005) showed that the Young's modulus increases with increasing age of the thrombi. In similar tests with different measurement methods (ultrasound-based in-vivo measurement) and different storage of the clotting thrombi, Mfoumou et al. (2014) showed lower values, although the correlation

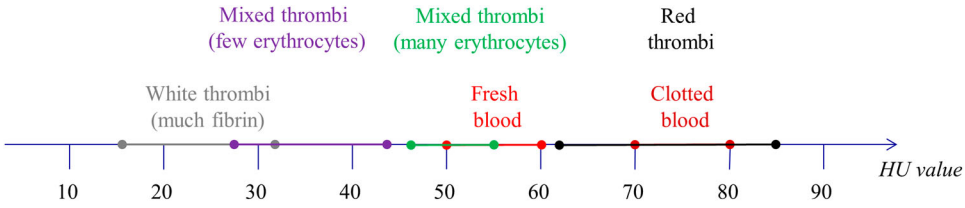

Figure 3. Hounsfield units of blood and thrombi according to (Mecke 2008; Vock and Woermann 2021).

of age and Young's modulus was also seen here. Using load-displacement curves, Slaboch et al. (2012) calculated the Young's modulus of thrombi and concluded that this was in the range of soft materials. From these studies, it can be deduced that a high fibrin content as well as increasing age make the thrombus stiffer and compact.

Johnson et al. (2017) describe high static friction of artificially created thrombi from animal blood in real animal blood vessels. Gunning et al. (2018) and Vidmar et al. (2015) investigated the friction between thrombus and vessel wall. Gunning et al. describe the resistance to sliding of the thrombus as friction. The coefficient of friction μ is defined as $\mu = \mathrm{Tan}\theta$, where θ is the angle of inclination, where the sample starts to slide on a low-friction surface (Gunning et al. 2018). They found that fibrin-rich thrombi have a significantly higher coefficient of friction than red thrombi (Vidmar et al. 2015; Gunning et al. 2018). This could explain the lower treatment success with fibrin-rich thrombi (Yuki et al. 2012).

In a study by Ryan et al. (1999) storage and loss modulus of human thrombi were investigated while varying the concentration of fibrinogen, thrombin, and solved calcium. The elastic fraction is determined by the storage modulus (G') and the viscous fraction by the loss modulus (G''). The loss modulus of white thrombi decreases with increasing fibrinogen concentration. With increasing thrombin concentration, the loss tangent also decreased. On the other hand, an increasing loss tangent was measured with increasing calcium concentration (Ryan et al. 1999).

The density of a thrombus is influenced by its composition. Generally, thrombus density is proportional to its precipitated calcium content. In addition, thrombus density may also increase by a growing number of cells (platelets and erythrocytes). After measuring 28 humans and 336 thrombi from 38 pigs Nahirnyak et al. found that the densities lie in the range of $(1.08 \pm 0.02) \times 10^3$ kg/m^3 for human clots and $(1.06 \pm 0.01) \times 10^3$ kg/m^3 for porcine clots (Nahirnyak et al. 2006). Thrombi thus are denser than blood (1.043–1.060 g/ml) (Vitello et al. 2015) On computer tomography imaging, the Hounsfield values also play a role. Figure 3 shows the value ranges for the different types of thrombi. Radiologists and Neuroradiologists rely on Hounsfield Units (HU) to quantitively evaluate the density of different substances on computer tomography. Thus, thrombi with a higher amount of precipitated calcium present with higher HU values in comparison to their softer, erythrocyte-richer counterparts (Walker et al. 2014).

With regard to the fragmentation properties of a thrombus, various studies show qualitatively that thrombi with a high proportion of erythrocytes (red thrombi) are more likely to fragment than fibrin-rich, white thrombi (Chueh et al. 2011, 2012; Vidmar et al. 2015; Johnson et al. 2017). According to Chueh et al. (2012), the stent retriever used also significantly influences thrombus fragmentation.

The interaction between thrombus and stent retriever was studied by Weafer et al. (2019) using the stent retriever EmboTrap MT device (Cerenovus, Galway, Ireland). It was shown that as the fibrin content increases, the time of integration of the thrombus into the stent retriever also increases (Weafer et al. 2019). When the erythrocyte content is increased, the time of integration of the thrombus into the stent-retriever decreases. Erythrocyte rich thrombi are easier to remove, but may fragment and cause distal emboli due to thrombus instability (Weafer et al. 2019).

Figure 4 summarizes the factors and relationships influencing the mechanical properties of thrombi.

Materials and methods

For the development of the synthetic thrombus models, a systematic approach based on VDI 2221 'Methodology for the development and design of technical systems and products' is chosen (Verein Deutscher Ingenieure e.V 2019). It is also a highly iterative process in which the results of the tests and thus

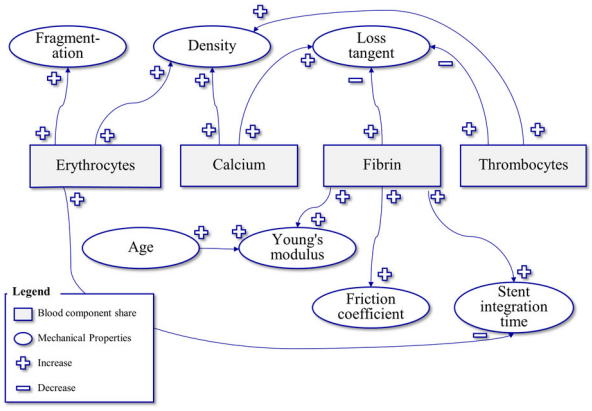

Figure 4. Thrombus mechanical properties – their correlations and influencing factors information based on (Ryan et al. 1999; Chueh et al. 2011, 2012; Vidmar et al. 2015; Johnson et al. 2017; Gunning et al. 2018; Weafer et al. 2019). + indicates an increase, while – shows a decrease (e.g. when the thrombocyte content increases, the density of the thrombus increases).

the feedback from the treating physicians is reflected back into the development. The HANNES model is the starting point for synthetic thrombi development and testing.

Hamburg anatomical neurointerventional simulator

In previous studies, the Hamburg Anatomical Neurointerventional Simulator (HANNES) for aneurysm treatment was developed in collaboration with the University Medical Center Hamburg Eppendorf (UKE) and has been described in detail in (Spallek et al. 2019). HANNES is a physical model that allows realistic simulations of neurovascular disease with real treatment tools (Nawka et al. 2020). HANNES is placed in the Hermann Zeumer Laboratory (HZL) at the UKE. The HZL provides a research environment with real operating room conditions. It consists of an operating table and an X-ray system 11Philips Allura Xper FD 20/20 with C-arm. Figure 5(a) shows HANNES in the experimental, realistic clinical environment at the HZL at UKE. The enlargement (b) shows the anatomical blood vessel models produced by Additive Manufacturing (AM).

As mechanical thrombectomy requires a similar operational setting as endovascular aneurysm treatment, the HANNES model could be extended to allow training of stroke treatment. The goal of HANNES is to create an animal-free simulation environment; therefore, the use of animal blood is also avoided for thrombi.

Identification of the requirements

Based on the defined objectives and the fundamentals of thrombectomy and thrombi, the requirements for a thrombus model are determined together with the neurointerventionalists and classified into the categories physical and functional.

The physical requirements (P) (see Table 1) are based on the mechanical parameters described in Chapter *Fundamentals*, as well as further geometrical and chemical requirements that a thrombus model must (D = demand) or should (W = wish) fulfil. Since it is not possible to define uniform values from the literature due to the diversity of the thrombi studied, these are quantified by value ranges.

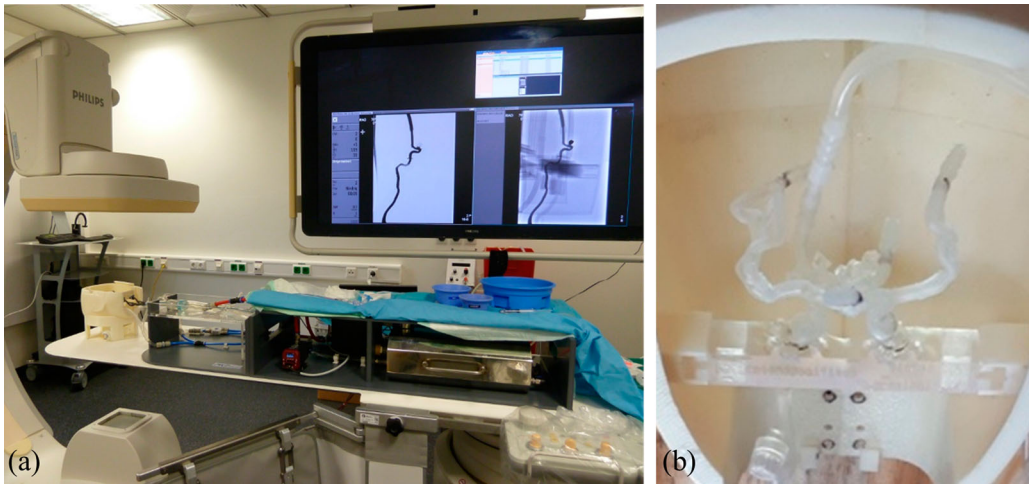

Figure 5. HANNES (a) in the clinical environment, (b) enlargement of the anatomical blood vessel model in the head

Table 1. Physical requirements for a synthetic thrombus model (D = demand), (W = wish).

Pos.	Physical requirement	Numerical value	D/W
P-1	Animal blood free	–	D
P-2	Usability in water	–	D
P-3	No toxicity	–	D
P-4	Low material hardness	~0 A	D
P-5	Young's modulus	5 - 100 kPa (Tendency rather at 5 - 30 kPa)	D
P-6	Geometry	Length = 6 - 15 mm Diameter = 1 - 3 mm	D
P-7	Tensile strength	10 kPa	W
P-8	Yield strength	300%	W
P-9	Density difference (blood/thrombus)	40 - 50 g/l	W
P-10	Loss tangent	0,02- 0,1	W
P-11	Durability	Min. 48 h	W

Table 2. Functional requirements for a synthetic thrombus model (D = demand), (W = wish).

Pos.	Functional requirement	D/W
F-1	Perforability (pierceability of the thrombus)	F
F-2	Fragmentation	F
F-3	No remaining adhesion, realistic haptics when retracting	F
F-4	Stent integration visible	F
F-5	Elasticity during retraction of the stent retriever low	W
F-6	Significant flow reduction (> 50%)	W
F-7	Visibility of the thrombus in the DSA	W
F-8	Simple manufacturability	F

The functional requirements (F) (see Table 2) are qualitative requirements that describe the behaviour of the thrombus in the training model and should be as close to reality as possible.

Due to the broad spectrum of different thrombi, the focus will be on four different thrombus variants, which can be differentiated in terms of firmness, into soft and hard, and in terms of breakability, into compact and fragile.

As described in Chapter *Fundamentals*, red thrombi are softer, more elastic and fragile as white thrombi. White thrombi, on the other hand are more adherent to vessel wall and thus, more difficult to retrieve. Very hard thrombi are usually associated with higher calcium fractions.

Conceptual design and material selection

The main function of the thrombus model is to 'reproduce thrombus in the training model' for training of operating physicians and device testing. This includes the realistic mapping of the described physical and functional properties, such as replicating thrombus stent integration, replicating adhesion to vessel wall model, and replicating fragmentation. In addition, the durability of the thrombus models plays a role.

Since all sub-functions can be achieved by certain material properties, a broad material selection is performed first. For this purpose, a material database is used. The CES Selector software (version 2012) from Granta Design Limited, Cambridge, UK, allows material charts to be created based on criteria. The procedure was based on the systematic material selection according to Ashby (2017). The physical requirements listed in Section *Identification of the requirements* serve as criteria for the search. In the first step, an overview analysis is carried out with all physical requirements, whereby no result was obtained. Then, three selections are performed, with the results of the previous selection forming the basis for the subsequent one (cf. Figure 6). The first selection (Figure 6(a)) is performed with Young's modulus and density, where foams (light green) and honeycomb structures (purple) under consideration of Young's modulus and elastomers (light blue) under consideration of density find themselves in the range of literature values. Materials made of paper, aluminium or glass/phenol are suggested as honeycomb structures, which are not suitable for the training model. Based on foams and elastomers, a further selection is performed. The limit for Young's modulus is set $\leq$ 0.001 GPa (cf. Figure 6(b)). 27 potential materials are proposed to enter the third selection. The requirements for tensile strength and hardness (ability of a material to resist indentation, scratching, or abrasion Cardarelli (2008), here in the form of the Vickers hardness) are used for this purpose. As a limit, the requirements 'usability in water' and 'non-toxic' are also added. Figure 6(c) shows the material diagram after the third selection. Foams are still shown in green and elastomers in light blue/red. This leaves 18 potential material solutions, which are listed in Table 3 in the form of 8 different materials due to their similarity.

The listed materials meet the requirements of usability in water, no toxicity as well as low hardness. The requirements for the Young's modulus, tensile strength and density difference cannot be completely fulfilled by any material. By sorting according to tensile strength and Young's modulus, polyurethane foams and melamine foams are closest to the requirements, so they will be investigated further.

The database mainly contains solids, so that other suitable materials, such as gels, etc., cannot be found by systematic material selection using the CES selector.

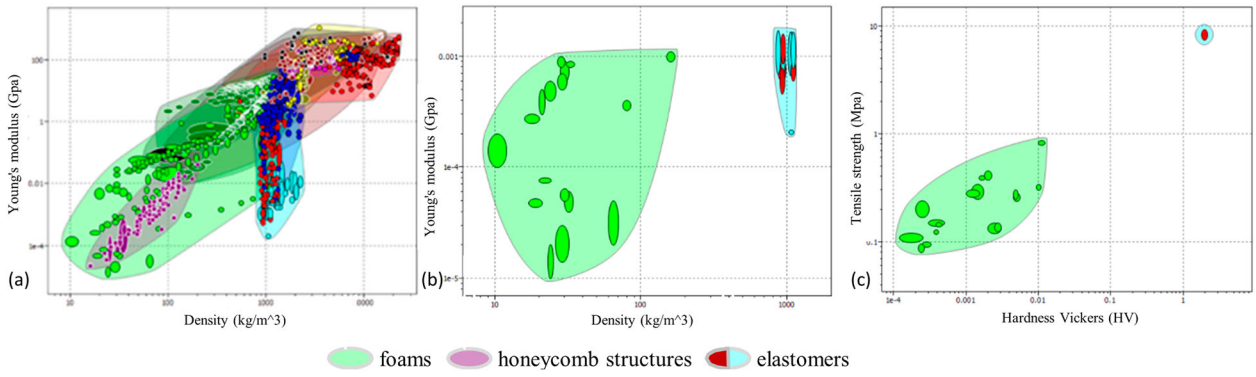

Figure 6. Material diagrams of the systematic material selection using the CES-Selector software. Narrowing down the materials according to (a) the first selection with young's modulus and density, (b) the second selection with Young's modulus $\leq$ 0.001 GPa and (c) the third selection with tensile strength and hardness – Vickers as well as 'usability in water' and 'non-toxic'.

Table 3. Extract from the material list of the CES selector after the third selection.

Material	Tensile strength [MPa]
Polyurethane filter foam (open-pored, 0.019)	0,08 - 0,095
Polyurethane foam (elastomer, open-pored, 0.065)	0,1 - 0,12
Melamine foam (0.011)	0,12 - 0,15
Polyurethane foam (flexible, fine-pored, 0.08)	0,125–015
Polypropylene foam (fine-pored, 0.020)	0,24 - 0,28
Polyethylene low density foam (cross-linked, fine-pored, 0.018)	0,26 - 0,3
Polyethylene high density foam (cross-linked, fine-pored, 0.030)	0,8 - 0,85
Polyvinyl chloride elastomer (Shore hardness A35)	7,43 - 9,25

By means of a literature search, further materials that have become established in biomedical applications could be identified. These include hydrogels (e.g. Bajpai and Shrivastava 2000; Petrini et al. 2003; Leiendecker 2017; Lingenhöhl 2017). In a study on clot traps, Robinson et al. (2013) use polyacrylamide to produce artificial blood clots. However, this fabrication involves a complicated chemical process and is therefore not pursued further (cf. Table 2).

In addition to the Puupsie, which was already used in radiographers courses, other commercially available children's play slimes are included in the analysis. These consist to a large extent of polyacrylates (polyacrylic esters). Gelatine is also commonly used in medical research (e.g. Betrouni et al. 2013; Liu et al. 2015; Carr et al. 2018). Agarose is the animal-free alternative to gelatine and is also frequently used in the field of phantom production (e.g. McIlvain et al. 2019). Silicone is also used as a substitute in the medical context. Among others, Paramasivam et al. (2014) investigate the use of silicone models for training and research in the field of endovascular neurointervention.

In addition to the materials described, an attempt is also being made to develop a thrombus model using structural properties. Additive Manufacturing (AM) is used for this purpose, as it offers a high degree of geometric freedom. The stereolithography process is chosen because it allows very small layer thicknesses and a high resolution due to a small laser focussing. The Form 2 and Form 3 printers form Formlabs, Sommerville, USA, are available. Due to production-related restrictions, only structures with a size of 0.5 mm or larger can be used.

Designing the structural thrombi using additive manufacturing

In addition to achieving thrombus requirements based on material properties, the possibility of structurally reproducing thrombus characteristics is being investigated. For this purpose, two structures are developed which should fulfil certain functional requirements and are based on the principle of the predetermined breaking point. First, a structure of small spheres is designed, and second, thin rods form a structure for the thrombus. The photopolymer Flexible Resin from the company Formlabs is used as the material (Formlabs 2021).

The first model consists of a cylinder occupied by spheres. It represents a very compact model. The face has a surface coverage of approximately 91%. The second model consists of spirals with thin bars forming the shape of a cylinder. Three curved cross struts provide additional stabilization in the central part of the

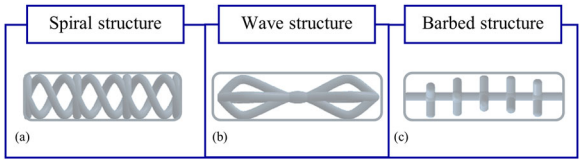

Figure 7. Design of the combined agarose thrombus model with stabilization by (a) a spiral structure, (b) a wave structure, (c) a barbed structure, additively manufactured (Wortmann et al. 2021).

model. The front face has a surface coverage of approx. 70%.

Other AM structures have been developed to be combined with agarose. These structures are intended to provide more stability to the agarose thrombi. These models have a length of 9 mm and a diameter of 2.5 mm and are made of Flexible Resin (Wortmann et al. 2021).

Following the model with the thin rods, a structure of spirals is designed, which has two symmetrical spirals and connected by an additional four rings with cross-connections (cf. Figure 7(a)). The cross-connection is intended to stabilize the model without strongly influencing the elasticity. The spirals and circles are intended to prevent compression of the agarose in the transverse direction, although compression in the longitudinal direction is possible. The cavity in the model should allow the thrombus to be pierced with the treatment instruments.

In addition to the structure of spirals, a wave structure is designed (cf. Figure 7(b)). The structure consists of three waves and a continuous bar. This results in three chambers which are filled with agarose. The structure was designed so that the model is stable against compression in the longitudinal and transverse directions, but allows for slight bending as well as perforation.

The third concept for the combination of agarose and AM support structure consists of a continuous elongated rod with barbs (cf. Figure 7(c)). For additional stability, the junctions are reinforced by spheres. Fragmentation of the agarose is to be reduced by the barbed structure by means of absorption of the loads in the transverse direction. The structure is designed to allow slight bending as well as perforation of the model.

In tests, all materials and structures are checked for functional requirements (see Chapter *Test procedure - Thrombectomy simulation*).

Manufacturing of the thrombus models

The production of the various thrombus models is described below. The agarose- and silicone-based thrombi as well as the additively manufactured thrombi have been patent pending (Wortmann et al. 2021). Food colouring (Günthart & Co. KG, Hohentengen, Germany) is added to some thrombus models to make them more distinguishable in the test.

Polyurethane foams: Polyurethane foams (density 18 kg/m^3, Shore hardness 25 A, flexolan® e.K., Diedorf, Germany and density 25 kg/m^3, compression hardness 40 kPa, Saarschaum GmbH & Co. KG, Kirkel, Germany) as well as melamine foam (board, Basotect density 9 kg/m^3, Saarschaum GmbH & Co. KG) cut into test specimens of 10 × 4 mm.

Slimes: The children's toy slimes are purchased from the company Simba Toys GmbH. The children's toy Slimy Puupsie is provided by drawing up approx. 0.2 ml in a heparin syringe (Omnifix-F from B. Braun SE, Melsungen, Germany). The children's toy Glibbi Slime is available as fine granules and is added to tepid water in the amount of 0.4% by weight according to the manufacturer's instructions. Since this results in a very liquid slime, the concentrations were increased to 5% by the weight of granules. The children's toy Glibbi Snowball is also available as granules and is poured over with tepid water. According to the manufacturer's instructions, 1 wt.% granules are dissolved in water. Since this appears very soft, an additional 2 wt.% solution is prepared.

Agarose: The agarose (Rotigarose, Carl Roth GmbH + Co. KG, Karlsruhe, Germany) was prepared in 2, 5 and 10 wt. %. The agarose is heated to above 95°C in a solvent and coloured with food colouring at a ratio of 0.1 g to 25 g. The mixture is cooled for 2 h. The preparation is carried out in two different ways. One is in a silicone tube (inner diameter 3 mm), the other is in the form of a block from which the thrombi were cut out (cf. Figure 8). After production, the agarose thrombi are stored in small tubes in an almost airtight manner to prevent the previously observed shrinkage of the material (Wortmann et al. 2021).

Before the agarose gelation process (at approx. 34–38°C), further additives can be added. This is used to add stabilizing components to the agarose.

As a stabilizing component, the agarose craft glue (C. Kreul GmbH & Co. KG, Hallerndorf,

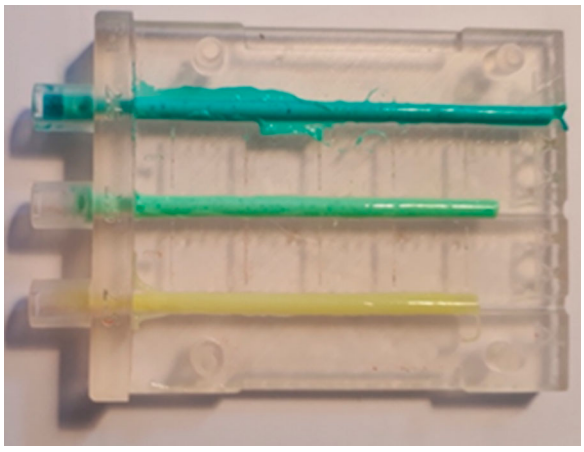

Figure 8. Preparation of agarose thrombi by casting into a home-made mould with a diameter of 2.5 mm.

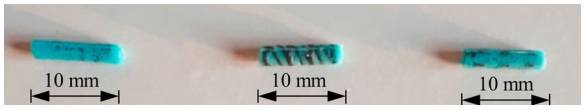

Figure 9. Combined thrombus models of AM structure and agarose stained with food colouring, (a) barbed structure, (b) spiral structure, (c) a wave structure.

Germany) was added. This consists of a 3:1 mixture of methylchloroisothiazolinone (MCI) and methylisothiazolinone (MI). These are used in the industrial sector as preservatives and binders in paints, lubricants and cosmetics, and serve as the main ingredient for water-soluble adhesives (Reinhard et al. 2001). This additive is believed to help reduce agarose fragmentation without reducing elasticity. For this purpose, 1, 2 and 5% agarose mixtures are prepared, to which in turn 5, 20 and 40 wt. % MCI + MI are added (Wortmann et al. 2021).

Gelatine: Powdered gelatine (material Aspic One A Quality 300 Bloom, MeinMetzger AG, Bad Orb, Germany) is mixed with warm water (approx. 35°C) in the ratio of 5 and 10 wt.% and cooled for 10 h.

Silicone: To produce a soft silicone with Shore A hardness of 0, an additive cold-crosslinking silicone elastomer (F ZA 00 (0 ShA) base and catalyst, Zhermack GmbH, Marl, Germany) is mixed with a base and catalyst in a ratio of 1–1 and cured for 12 h. In addition, to achieve a softer mixture, a ratio of 3 ml base to 2 ml catalyst is selected.

On the one hand, the silicone thrombi are produced in a specially developed mould. The silicone thrombi have a diameter of 2.5 mm and a length of 9–11 mm. On the other hand, the liquid silicone mixture is drawn into a 1 ml syringe (Omnifix-F from B. Braun SE, Melsungen, Germany) with a cone diameter of 2.1 mm and a cylinder diameter of 5.0 mm for curing. After curing, the silicone is pressed out of the syringe.

The mixing and curing process offers the possibility to influence the properties of the silicone by changing the mixing ratio of base and catalyst or by adding further components to the mixture.

In order to change the elasticity and stickiness of the silicone, the mixing ratio of base and catalyst is varied. Mixtures with a 10–50% base content are produced.

To influence the properties, craft glue (MCI + MI, C. Kreul) was added to the silicone thrombi as described for the agarose thrombi. This is done for silicone thrombi with a base fraction of 30% and 40%, which were supplemented with 20, 30, 50, and 60 wt. % MCI + MI, respectively.

To increase the fragmentation property, micro-glass pearls (MGP) from Carl Roth GmbH + Co KG, Karlsruhe, Germany, with a diameter of 0.25–0.5 mm were added to the silicone thrombi (Wortmann et al. 2021).

In addition, silicone thrombi are stored in vegetable oil to reduce their stickiness.

AM structures: The structural models are produced using the Form 2 and 3 printers (Formlabs) in the Photopolymer Flexible Resin material (Formlabs). After printing, the model is post-processed according to the manufacturer's instructions. Both cured and uncured models are produced.

For the preparation of the combined thrombus models from AM-prepared structures and agarose, proceed as follows: The structures are fabricated as described above. They are then placed in the specially developed mould and cured with an agarose mixture for 12 h. These thrombus models are subsequently stored in small airtight tubes. Figure 9 shows the agarose thrombi with the different support structures.

Porcine blood thrombi: For the first test series (see Section *Preliminary tests for limiting the materials*), porcine whole blood thrombi were used as a reference for the assessment of functional properties. For this purpose, thrombin (Thrombin Reagenz from Siemens Healthcare Diagnostics) is dissolved in Aqua Dest (Aqua ad iniectabilia from B. Braun, Melsungen, Germany) and filled into a heparin syringe. Barium sulfate and porcine blood (10 ml) are filled into a Luer lock syringe (Becton Dickinson GmbH, New Jersey, USA)

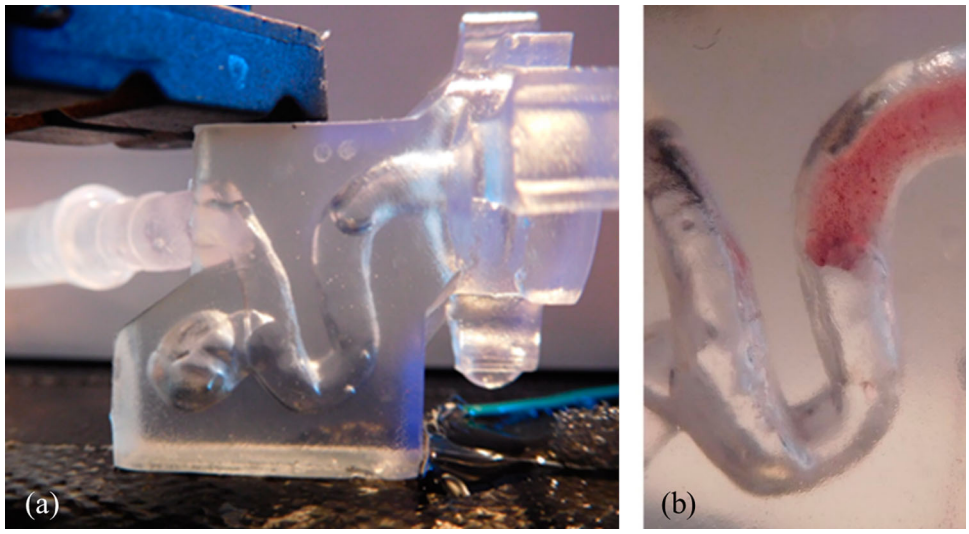

Figure 10. Test environment for the first preliminary tests to narrow down the materials. An intracranial aneurysm model was printed from a block of clear resin on Formlabs Form 2 (a), coloured silicone thrombus (base 3: catalyst 2) in the test environment (b).

and the thrombin solution is added. The mixture is swirled in a Heidelberg extension (Fresenius SE & Co. KGaA, Bad Homburg vor der Höhe, Germany) (3 mm inner diameter) and allowed to settle for at least 10 min. In the present test, the clotted blood is kept refrigerated in the Heidelberger extension for 24 h. The clotted blood is then placed in saline (0.9% NaCl) and the thrombi are cut into pieces approximately 10 mm long.

Test procedure – thrombectomy simulation

The experiments are divided into a preliminary test, in which a large number of materials are tested in a simple experimental setup, with the aim of narrowing down the number of materials. Porcine whole blood thrombi are used as a reference for this selection. Based on this selection, qualitative tests will be performed on HANNES with neuroradiologists of the UKE. In a further series of tests at HANNES, three tests will be carried out with the aim of classifying thrombus models into the four defined categories.

Preliminary tests for limiting the materials

In the preliminary tests, the functional requirements (F) (see Section *Identification of the requirements*) are checked using a simple set-up. For this purpose, the test bodies are prepared as described in Section *Manufacturing of the thrombus models*. The test bodies are portioned using a heparin syringe. The foams are cut using a scalpel. The test environment represents a carotid siphon model based on patient-specific 3D DSA data, which was produced as a block on Form 2 in the material Clear Resin (Formlabs) (see Figure 10). The transparent material is chosen to achieve good visibility of the process steps of a thrombectomy in the test, although ideal properties in terms of friction are not achieved with this material.

The test body is flushed into the model with water. If this is not possible, it is advanced mechanically. A thrombectomy is simulated with the guidewire Hybrid Wire (Balt, Montmorency, France), the microcatheter Rebar-027 Micro Catheter (Micro Therapeutics, Inc., Irvine, USA) and the stent retriever ERIC 3 (MicroVention, Inc., Aliso Viejo, USA). Flow reduction, perforation of the thrombus (which also includes advancing past the thrombus), stent integration, resistance to stent retrieval, elasticity of the thrombus, adhesion to the vessel wall, and fragmentation of the thrombus will be assessed. As a first approximation, the porcine whole blood thrombi presented in Section *Manufacturing of the thrombus models* are used as a reference. These are two thrombi each with 5% thrombin, with and without barium sulfate.

Tests on HANNES

Further testing of a narrower range of materials will be performed at the HZL on the HANNES model with three neuroradiologists (HG, AAK, AMF). Water with

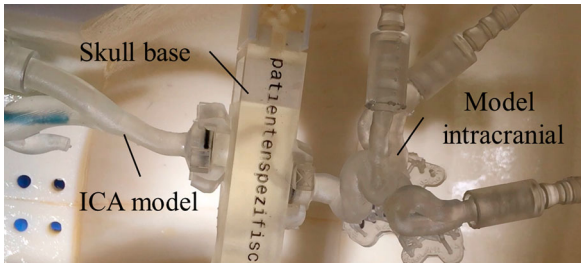

Figure 11. Blood vessel models in the HANNES model in the first and second test. The skull base is made of Clear Resin (Formlabs) and the ICA and intracranial model are made of Elastic Resin (Formlabs).

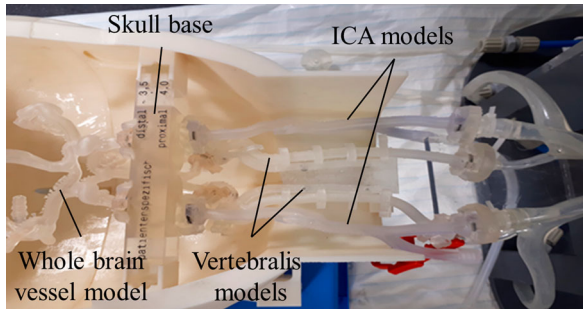

Figure 12. Whole-brain vessel model in HANNES for the final test series. For this purpose, another ICA model was connected as well as the posterior cervical arteries, the vertebral models.

commercially available soap is used as blood substitute in HANNES.

In a first test at HANNES, the materials Slimy Puupsie from Simba Toys and agarose are tested in concentrations of 2 and 5%. For the production of the agarose, on the one hand a silicone tube is used for curing, on the other hand the agarose is cured and cut as a block. The test bodies ($d = 3$ mm, $l = 8$ mm) are introduced via the guide catheter (7 French), which is advanced into the anterior neck artery, and transported further distally with blood flow until occlusion occurs. A whole brain vessel model out of Elastic Resin (Formlabs) was used.

In further test series at HANNES with the medical experts at the UKE, three tests will be carried out. The criteria elasticity, adhesion and fragmentation are used to evaluate the thrombus models.

In the first and second test, a patient-original vessel model consisting of carotid siphon with carotid T and A. cerebri media and A. cerebri anterior is used intracranially (cf. Figure 11). The vessel model is made of Elastic Resin (Formlabs). An additional vascular branch is be added to the internal carotid artery (ICA) model (Elastic Resin) to allow vascular insertion of the agarose thrombus models. In the first series of tests, silicone thrombi ($d = 2.5$ mm, $l = 9$–11 mm) are tested from the mould and with and without prior storage in oil. These are applied via the guide catheter. In the second series of tests, thrombus models from agarose with MCI + MI ($d = 2.5$ mm, $l = 11$ mm) are tested. The application is performed via the additional vascular branch.

The third experiment represents the final test. Here, silicone-based thrombi with micro-glass pearls and agarose-based thrombi with support structures were tested. A whole-brain vessel model depicting the anterior and posterior circulation was used as the vessel model (cf. Figure 12). The neck arteries as well as the whole-brain vessel model are made of the material Flexible 80 A (Formlabs), as this material, which has just become available at the time of the experiments, shows promise for the replication of vessels due to its properties (higher stability and better manufacturing accuracy). A filter is placed downstream of the whole-brain vessel model to filter out possible thrombus material. The thrombus is introduced via the additional vascular branch. Eight thrombus models ($d = 3$ mm) based on agarose and silicone are tested. Agarose-based thrombus models are prepared by 2% agarose in combination with 10% and 20% MCI + MI. Another model is the combination of 2% agarose with 10 wt. % MCI + MI and the AM-produced wave structure. As silicone-based thrombus models, on the one hand, a base portion of 30% is combined with an addition of MCI + MI of 30% and stored in oil. On the other hand, models with 30% silicone base are combined with 30% and 40% MCI + MI. Furthermore, 10 and 30 wt. % micro-glass pearls are added to the mixture.

Results and discussion

In the search for suitable thrombus replacement materials, findings were obtained during material production, from preliminary in vitro testing using a vascular model as well as evaluations performed by experienced neurointerventionalists from the UKE on the HANNES simulation model. For an evaluation from a clinical perspective, see also (Guerreiro et al. 2021).

Results from the production and preliminary test

Due to their properties being too liquid or too soft, the materials Glibbi Slime with 0.4% by weight, Glibbi

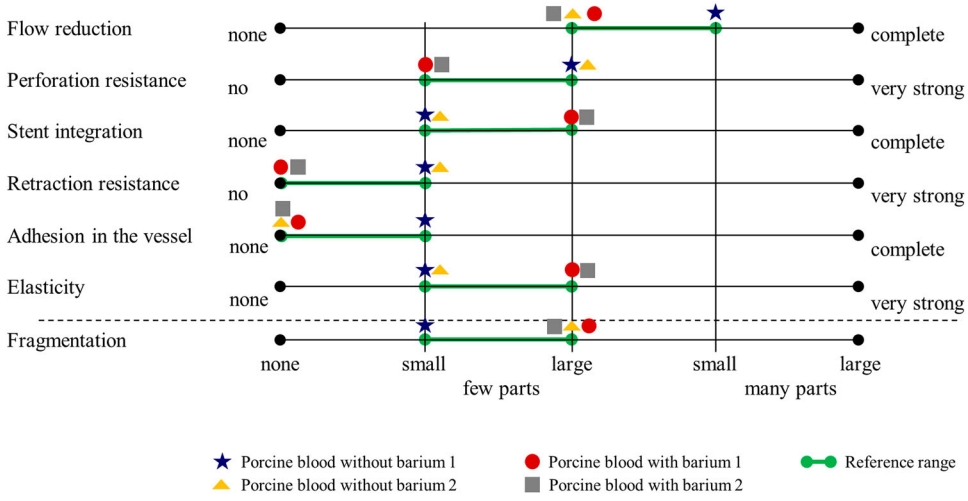

Figure 13. Qualitative evaluation of various parameters using porcine blood thrombi with and without barium. The reference range (green) was derived from this.

Snowball with 1% by weight and gelatine with 1% by weight are already excluded during production.

Reference from porcine whole blood thrombi: For further investigation of materials that could be used for thrombus simulation, a subjective reference standard for the evaluation of thrombi needed to be defined. As not all thrombi are the same, an acceptable range was used. Reference ranges are established by simulating thrombectomy with porcine blood thrombi (see Figure 13, green). A 5-level scale is used to semi-quantitatively assess the evaluation criteria. The thrombi show moderate to advanced flow reduction in the vascular model, mild to moderate perforation resistance, mild to moderate detectable stent integration, no or low resistance to stent retrieval, no or mild adhesion in the vascular model, mild to moderate elasticity, and mild fragmentation (cf. Figure 13).

Thrombus models from AM printed structures: The structure with the spheres is not perforable with the microcatheter in both hardened and unhardened forms, so this structure is shown to be unsuitable for thrombectomy. The structure with the rods in unhardened form also fails to achieve perforation. However, the structure with rods in hardened form could be perforated. No significant flow reduction is achieved with any of the models. The models also fall outside the defined reference range for the other criteria. Therefore, these models are excluded for the replication of a thrombus.

Thrombus model from foams: Neither flow reduction nor perforation could be achieved with the test body made of melamine foam. The test body made of polyurethane foam also produced no flow reduction, whereas perforation, stent integration and retraction resistance were within the reference range. PUR foams, on the other hand, show no elastic behaviour and do not fragment, so that they are also excluded as a substitute material.

Silicone based thrombus models: Silicone thrombus with a 3 base to 2 catalyst ratio can only meet the requirement of perforation resistance. Silicone with a 1:1 ratio, on the other hand, is within the reference range in flow reduction, stent integration, retraction resistance, and fragmentation. However, this model could not be completely removed with the stent retriever, and the perforation resistance is also very high. Therefore, these pure silicone thrombus models are more suitable for replication for very compact and hard thrombi.

Agarose-based thrombus models: The agarose thrombus with 10% concentration could not be removed with the stent retrievers. The 5% agarose thrombus is within the reference range for the criteria of perforation resistance, stent integration, retraction resistance, adhesion in the vessel model, and fragmentation. However, for flow reduction and elasticity, it is below the reference range. It can be observed that with increase in agarose concentration, the strength of the test body increases. It becomes more compact. As a result, the stent integration decreases.

Two percent agarose is in the reference range for flow reduction, but the perforation resistance was

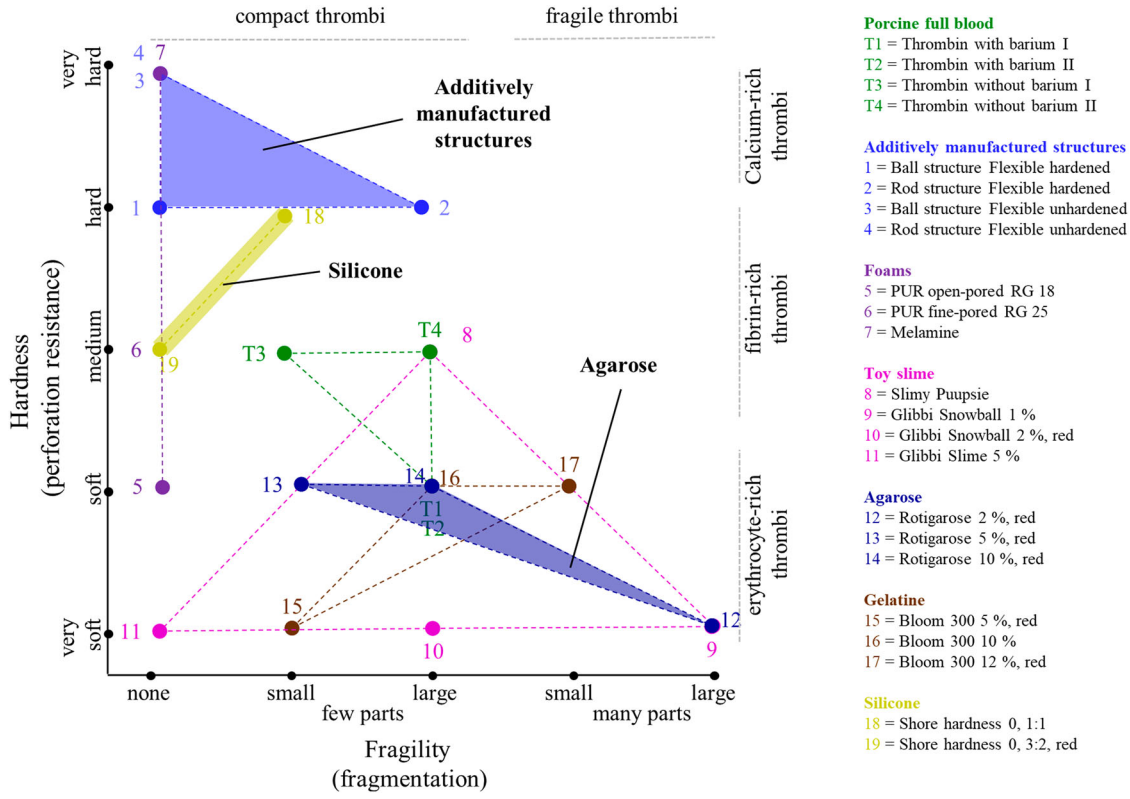

Figure 14. Graphical evaluation of the potential thrombus material classes with respect to their fragility and hardness after the preliminary tests. The favourites were highlighted in medium blue, dark blue and light green.

found to be lower. The stent integration is also estimated to be slightly stronger. The previous problem of agarose is the lack of resistance to mechanical stress, especially compression leads to unrealistically high fragmentation.

Gelatine-based thrombus models: With increasing gelatine concentration, perforation resistance as well as flow reduction increases. Stent integration was best with the 10% test specimen.

Gelatine was included in principle as a comparison to the properties with agarose, but it is not an alternative as a replacement material in the HANNES training model because it is not animal ingredient free. Therefore, it will not be investigated further.

Thrombus model from Simba Toys test bodies: Glibbi Slime 5% and Glibbi Snowball 1% show a clearly too high stent integration compared to the porcine whole blood thrombi. Glibbi Snowball 2%, Slimy Puupsie and Glibbi Slime 5% show unrealistic elongation behaviour. In addition, Glibbi Slime and Snowball showed slight liquefaction in contact with water. Slimy Puupsie achieves good results in the area of flow reduction, perforation resistance as well as fragmentation.

In summary, the results for the preliminary tests are shown in Figure 14 based on the criteria of hardness and fragility. In order to achieve the thrombus variants targeted in Section *Identification of the requirements*, it is necessary to optimize the suitable materials with respect to these criteria. This was done in Section *Tests on HANNES*.

Results from tests on HANNES

In the first test at HANNES, agarose thrombi and Slimy Puupsie were tested and compared. Based on the results, a series of experiments consisting of three trials was performed.

Testing of agarose thrombi in HANNES

Agarose thrombi do not achieve complete flow reduction. Contrast medium penetrates the test body or flows past it, so that the test body becomes visible in the angiography (cf. Figure 15). The 2% agarose thrombus fragments already during induction, which is further enhanced by contact with the microcatheter. High fragmentation on flushing is seen in the 5% round thrombus model. The stamped models of the

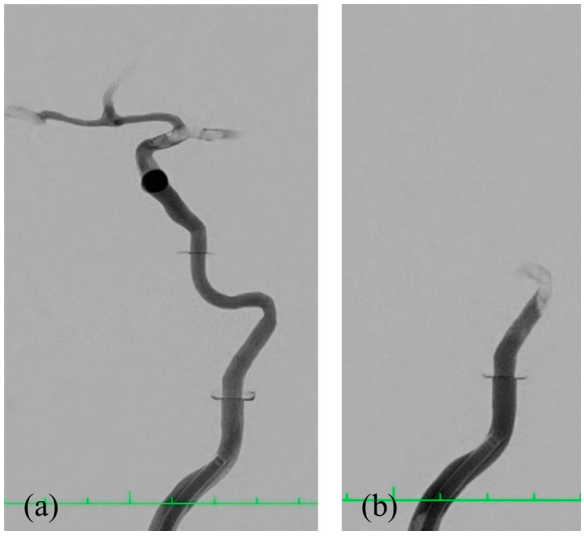

Figure 15. Visualization by angiography and contrast medium. Occlusion of the A. cerebri media by a stamped test body of 2% agarose (a) and occlusion of the skull base by a stamped test body of 5% agarose (b).

same composition fragment only upon contact with the microcatheter. The stent retriever is pulled through the test body, so no stent integration is observed.

The Slimy Puupsie material shows excessive elastic behaviour, complete stent integration and no fragmentation.

Test series on HANNES

The series of tests on HANNES are carried out in three trials. In test 1, different compositions of silicone with stabilizing components (see *Manufacturing of the thrombus models*) are tested in HANNES. The second test includes the test of different agarose thrombi. The third test represents the final test, which again tests the favoured models across each other. Table 4 summarizes the results of the first experiments.

It is shown that silicone thrombi with a base content of 40% are too compact, so that they are excluded as replacement material. Thrombus models with a base content of 30% and an addition of 30 or 50 wt.% MCI+MI show promising behaviour. An increase in elasticity with the addition of MCI+MI was observed. With previous storage of the models in oil, a decrease in adhesion as well as a slight increase in fragmentation could be observed.

The silicone thrombi rather represent the behaviour of soft and compact thrombi, which fragment predominantly under significant mechanical stress.

Table 4. Results from the first test of the series of tests on HANNES.

Model ID	Composition	Observation
B3-KL20	30% base content 70% catalyst + 20 wt.% MCI + MI	Low elasticity Moderate adhesion (rolling) Small fragments in stent retriever, majority aspirated
B3-KL30	30% base content 70% catalyst + 30 wt.% MCI + MI	Elasticity moderate Significant adhesion Complete closure Direct aspiration successful
B3-KL30-oil	30% base content 70% catalyst + 30 wt.% MCI + MI stored in oil	Moderate elasticity Reduced adhesion Complete closure Fragmentation into two fragments, recovery successful
B3-KL50	30% base content 70% catalyst + 50 wt.% MCI + MI	Elasticity high Moderate adhesion Complete closure Direct aspiration No fragmentation
B3-KL50-oil	30% base content 70% catalyst + 50 wt.% MCI + MI stored in oil	Reduced adhesion High elasticity Recovery by aspiration
B4-KL20	40% base content 60% catalyst + 20 wt.% MCI + MI	Very compact Low elasticity Low adhesion No fragmentation Poor recovery
B4-KL30	40% % base content 60% catalyst + 30 wt.% MCI + MI	Very compact Low adhesion No fragmentation Elasticity moderate Recovery by stent retriever not possible
B4-KL50	40% base content 60% catalyst + 50 wt.% MCI + MI	Adhesion low Elasticity low No fragmentation

The results of the second tests with agarose thrombi are summarized in Table 5.

The agarose thrombi show little elasticity and no adhesion. They show a strong fragmentation behaviour. Models with 5% agarose fragment very strongly already when added to the model. Addition of MCI+MI to 2% agarose increases fragmentation, with 5–20 wt.% judged to be realistic, very fragile thrombi.

In the third experiment, the preferable clots from the previous two experiments are tested on HANNES. The results are shown in Table 6.

The addition of micro-glass pearls leads to a slight increase in fragmentation and stronger adhesion to the vessel model.

The silicone model with 30% base content, 40 wt. % MCI+MI and 10 wt. % micro glass pearls is classified as a soft and fragile thrombus. The silicone thrombus with a base fraction of 30%, an addition of 30 wt. %

Table 5. Results from the second test of the series of tests on HANNES.

Model ID	Composition	Oberservation
A1-KL05	1% agarose + 5 wt.% MCI + MI	Fragments into small fragments at insertion
A2-KL05	2% agarose + 5 wt.% MCI + MI	Encircled occlusion On exploration, the thrombus loses a small fragment Retrieved with stent retriever Thrombus shears off at the guiding catheter
A2-KL20	2% agarose + 20 wt.% MCI + MI	Encircled occlusion Displacement of the thrombus as well as significant fragmentation by microcatheter Retrieval partly with aspiration, partly with stent retriever
A2-KL40	2% agarose + 40 wt.% MCI + MI	Surrounded closure Very strong fragmentation before and during exploration
A5-KL05	5% agarose + 5 wt.% MCI + MI	Initially complete occlusion, slight fragmentation distally; then thrombus flowed around Complete fragmentation with stent retriever
A5-KL20	5% agarose + 20 wt.% MCI + MI	Significant fragmentation upon injection Encircled occlusion Strong fragmentation also during exploration
A5-KL40	5% agarose + 40 wt.% MCI + MI	Complete closure Very strong fragmentation

MCI+MI, and prior storage in oil is shown to be suitable to represent a soft and compact thrombus in the training model. The silicone thrombus with 40% base content and the addition of 20 wt. % MCI+MI can be considered as a hard and compact thrombus.

The agarose thrombi show a very strong fragmentation behaviour. The AM-produced wave structure gives more stability to the agarose thrombus, approaching a hard and fragile thrombus. However, the waved structure could not be recovered with the stent retriever in the test. Figure 16 summarizes the results for the types of thrombi to be obtained.

Discussion of the results

The tests have shown that it is possible to produce thrombus models on an agarose and silicone basis which, in terms of their behaviour during thrombectomy, fall within the range of real thrombi. The aim is not to exactly mimic the mechanical properties of animal blood thrombi, but rather to model the behaviour of the thrombus models in the training model HANNES to the haptic features during thrombectomy in humans.

Table 6. Results from the third test of the series of tests on HANNES.

Model ID	Composition	Observation
B3-KL30-oil	30% base content 70% catalyst + 30 wt.% MCI + MI stored in oil	Soft and compact No adhesion Recovery by stent retriever and aspiration good Small fragments remain in the stent retriever
B3-KL30-GP30-oil	30% base content 70% catalyst + 30 wt.% MCI + MI + 30 wt.% MGP stored in oil	Soft and compact Small fragmentation due to stent retriever Thrombus detaches from stent retriever and creates new occlusion
B3-KL40-GP10-oil	30% base content 70% catalyst + 40 wt.% MCI + MI + 10 wt.% MGP stored in oil	Soft and easily fragmenting No adhesion Recovery well possible Three large fragments in aspirate
B3-KL40-GP30-oil	30% base content 70% catalyst + 40 Gew.% MCI + MI + 30 Gew.% MG stored in oil	Soft and compact Strong rolling of thrombus between vessel wall and stent retriever Small fragments in the stent retriever
B3-KL40-GP30-syringe	30% base content 70% catalyst + 40 wt.% MCI + MI + 30 wt.% MGP from the syringe	Soft and moderately fragile Rolling of the thrombus Fragmentation on guiding catheter; fragments could be aspirated
A2-KL10	2% agarose + 10 wt.% MCI + MI	Very fragile Very difficult to retrieve Most of the thrombus is flushed out of the system No interaction between thrombus and stent retriever
A2-KL10-wave	2% agarose + 20 wt.% MCI + MI Support structure (wave)	Soft, moderately fragile casing with firm inner structure Recovery possible up to the guiding catheter, aspiration of the casing there; support structure not removable
A2-KL20	2% agarose + 20 wt.% MCI+ MI	Very strong fragmentation during insertion and exploration

Various factors influencing the behaviour of the thrombi in the training model were identified. Thus, in the first tests, simplified vascular models were used, which only depicted the carotid siphon with carotid T and A. cerebri media as well as A. cerebri anterior (two distal outlets). In the final experiment, a whole-brain vascular model was used, connecting the anterior, posterior, and left and right circulation, resulting in five distal outlets. Here, the use of the same pulsatile pump results in a different pressure distribution to each vascular model section. In addition, the skull base model was changed due to leakage from the preliminary tests to the main test, so that the distal diameter was reduced from 4.0 mm to 3.5 mm.

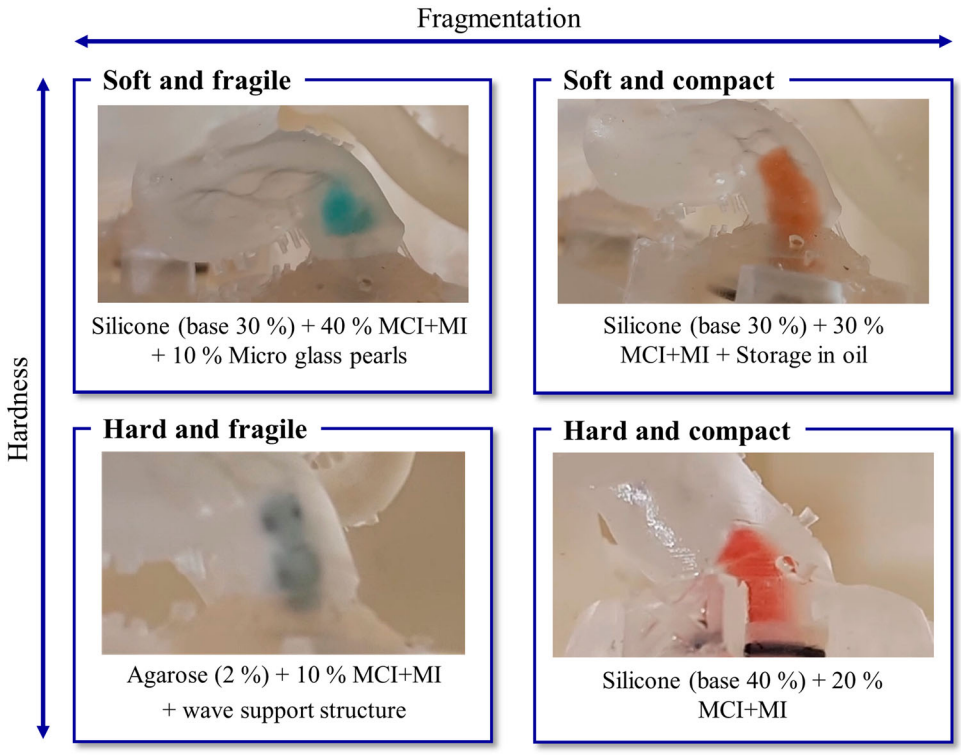

Figure 16. Selection and classification of thrombus models based on the properties of hardness and fragmentation in the defined categories.

Furthermore, an alteration on the vessel model material is also implemented, since with the Flexible 80A of the company Formlabs a new, promising material was introduced at the time of the test series. This resulted in an exchange from Elastic Resin in the first instances of the test series to Flexible 80 A in the final test. Whether this contributes to stronger adhesion, needs to be clarified in further investigations. It was also observed that the thrombus models stored in oil showed a reduced adhesion in the Elastic Resin vascular models, in contrast to the models not stored in oil. In contrast, in the Flexible 80 A vessel models, storage in oil appears to impair the integration of the thrombus in the stent retriever.

The appropriate behaviour of the agarose thrombi from the second test of the series of tests could not be reproduced in the final test. This could be due to the change in the diameter of the thrombus models from 2.5 mm to 3 mm as well as the changed experimental setup described above. With the change in diameter, a clear increase in fragmentation at the skull base can be observed.

Furthermore, it was observed that the guidewire did not pierce directly through the thrombus models, but instead shifted these slightly as it was guided past the thrombus. This causes a release of the stent retriever next to the thrombus. However, this mechanical behaviour of thrombus can also be observed during mechanical recanalization in patients.

The criteria evaluation was based on the clinical experience of physicians. This is a subjective impression that does not allow an objective assessment. Nevertheless, on the basis of experience, an assessment of the effects of added additives in agarose and silicone can be made and thus a tendency for the four types of thrombi can be derived. In particular, it can thus be shown that the manufacturing method (mould vs. syringe) has an influence on the properties. Also, the addition of MCI + MI contributes to an increase in elasticity and the addition of micro-glass pearls to an increase in fragmentation (Wortmann et al. 2021).

Summary and outlook

After extensive material selection and testing, development of four different thrombus models representing the four pre-defined thrombi types (soft and compact, soft and fragile, hard and compact, hard and fragile) could be successfully achieved. These show a realistic

behaviour. Optimization potential is shown for the soft, fragile thrombi. Their fragmentation properties need to be further improved in order to reproduce very fragile thrombi. Agarose thrombi could be considered for this purpose, which will be further optimized. The hard and compact thrombi, on the other hand, already show realistic behaviour and can be used for thrombectomy training in the training model. For the hard, fragile thrombi, further development of the AM-manufactured support structure will be necessary to make salvage via stent-retriever. This would allow soft thrombi with calcium content to be replicated.

For further analysis, the various thrombus models will be evaluated on the HANNES training model under constant conditions by a larger number of different treating neuroradiologists, in the setting of mechanical thrombectomy simulation, using a qualitative classification scale, as well as by means of quantitative measurement variables.

Ethics approval

Ethical approval for the retrospective patient data collection and analysis as well as the use of porcine blood was waived by the local ethics committee (Hamburg Medical Board, WF-068/21, Animal test number A10/657 and A2018/001).

Data availability statement

The data that support the findings of this study are openly available in Thrombus – Experiments at https://doi.org/10.15480/336.3773.

Acknowledgements

The authors would like to thank Philips Healthcare for the support and realization of the 'Hermann Zeumer Research Laboratory' including a Philips Allura Clarity Angiography system.

Disclosure statement

The described synthetically produced clots and their applicability in a neurovascular simulation situation were filed for patent with the German Patent Office under the reference 10 2021 112 467.0 on 12.05.2021 under the name 'Synthetisches Thrombusmodell zum Erlernen der operativen Entfernung eines Blutgerinnsels im Rahmen einer Behandlungsnachstellung' [Synthetic thrombus model for learning the surgical removal of a blood clot in the context of a treatment readjustment] (Wortmann et al. 2021). Outside of the submitted work Dr. Fiehler reports grants and personal fees from Acandis, grants and personal fees from Cerenovus, grants and personal fees from Medtronic, grants and personal fees from Microvention, personal fees from Penumbra, and personal fees from Phenox outside the submitted work; shareholder Tegus, CEO Eppdata.

Funding

This work was supported by the Federal Ministry of Education and Research – BMBF under [grant number 161L0154].

ORCID

Nadine Wortmann http://orcid.org/0000-0001-8640-1881
Helena Guerreiro http://orcid.org/0000-0003-0221-8954
Anna A. Kyselyova http://orcid.org/0000-0002-8662-0811
Andreas M. Frölich http://orcid.org/0000-0002-0804-1056
Jens Fiehler http://orcid.org/0000-0001-8533-7478
Dieter Krause http://orcid.org/0000-0002-1253-1699

References

Ashby MF. 2017. Materials selection in mechanical design. Oxford, UK: Butterworth-Heinemann an imprint of Elsevier.

Ashton JH, Vande Geest JP, Simon BR, et al. 2009. Compressive mechanical properties of the intraluminal thrombus in abdominal aortic aneurysms and fibrin-based thrombus mimics. J Biomech. 42:197–201. doi:10.1016/j.jbiomech.2008.10.024.

Bajpai AK, Shrivastava M. 2000. Dynamic swelling behavior of polyacrylamide based three component hydrogels. J Macromolecular Sci. Part A. 37:1069–1088. doi:10.1081/MA-100101141.

Berkefeld J. 2018. Mechanische Rekanalisation beim akuten Schlaganfall: [Mechanical recanalisation in acute stroke]. Radiologie up2date. 18:319–336. doi:10.1055/a-0657-7035.

Berkefeld J, Du Mesnil de Rochemont R, Sitzer M, et al. 2005. Mechanische Rekanalisation beim akuten Schlaganfall: [Mechanical recanalisation in acute stroke] [Mechanical recanalization in acute stroke treatment]. Radiologe. 45:455–460. doi:10.1007/s00117-005-1203-4.

Berkhemer OA, Fransen PSS, Beumer D, et al. 2015. A randomized trial of intraarterial treatment for acute ischemic stroke. N Engl J Med. 372:11–20. doi:10.1056/NEJMoa1411587.

Betrouni N, Nevoux P, Leroux B, et al. 2013. An anatomically realistic and adaptable prostate phantom for laser thermotherapy treatment planning. Med Phys. 40:22701. doi:10.1118/1.4788673.

Boodt N, van Snouckaert Schauburg PRW, Hund HM, et al. 2021. Mechanical characterization of thrombi retrieved with endovascular thrombectomy in patients with acute ischemic stroke. Stroke. 52:2510–2517. doi:10.1161/STROKEAHA.120.033527.

Brinjikji W, Nogueira RG, Kvamme P, et al. 2021. Association between clot composition and stroke origin in mechanical thrombectomy patients: analysis of the stroke

thromboembolism registry of imaging and pathology. J Neurointerv Surg. 13:594–598. [accessed 2021 Dec 3]. doi:10.1136/neurintsurg-2020-017167.

Cardarelli F. 2008. Materials handbook: a concise desktop reference, 2nd ed. London: Springer London. doi:10.1007/978-1-84628-669-8.

Carr DJ, Stevenson T, Mahoney PF. 2018. The use of gelatine in wound ballistics research. Int J Legal Med. 132:1659–1664. doi:10.1007/s00414-018-1831-7.

Chueh JY, Wakhloo AK, Gounis MJ. 2012. Effectiveness of mechanical endovascular thrombectomy in a model system of cerebrovascular occlusion. AJNR Am J Neuroradiol. 33:1998–2003. doi:10.3174/ajnr.A3103.

Chueh JY, Wakhloo AK, Hendricks GH, et al. 2011. Mechanical characterization of thromboemboli in acute ischemic stroke and laboratory embolus analogs. AJNR Am J Neuroradiol. 32:1237–1244. doi:10.3174/ajnr.A2485.

Formlabs. 2021. Using Flexible Resin V2 [Internet] [cited 2021 May 6]. https://support.formlabs.com/s/article/Using-Flexible-Resin-V2?language = en_US.

Gizewski ER. 2014. Mechanische thrombektomie: [Mechanical thrombectomy]. Wien Klin Mag. 17:32–39. doi:10.1007/s00740-014-0193-0.

Goyal M, Demchuk AM, Menon BK, et al. 2015. Randomized assessment of rapid endovascular treatment of ischemic stroke. N Engl J Med. 372:1019–1030. doi:10.1056/NEJMoa1414905.

Gralla J, Schroth G, Remonda L, et al. 2006. A dedicated animal model for mechanical thrombectomy in acute stroke. Am J Neuroradiology [Internet]. 27:1357–1361. http://www.ajnr.org/content/ajnr/27/6/1357.full.pdf.

Guerreiro H, Wortmann N, Andersek T, et al. 2021. Novel synthetic clot analogs for in-vitro stroke modelling; under submission.

Gunning GM, McArdle K, Mirza M, et al. 2018. Clot friction variation with fibrin content; implications for resistance to thrombectomy. J Neurointerv Surg. 10:34–38. doi:10.1136/neurintsurg-2016-012721.

Johnson S, Duffy S, Gunning G, et al. 2017. Review of mechanical testing and modelling of thrombus material for vascular implant and device design. Ann Biomed Eng. 45:2494–2508. doi:10.1007/s10439-017-1906-5.

Jovin TG, Chamorro A, Cobo E, et al. 2015. Thrombectomy within 8 h after symptom onset in ischemic stroke. N Engl J Med. 372:2296–2306. doi:10.1056/NEJMoa1503780.

Krasokha N, Theisen W, Reese S, et al. 2010. Mechanical properties of blood clots - a new test method. Mat.-Wiss. u. Werkstofftech. 41:1019–1024. doi:10.1002/mawe.201000703.

Kreusch A. 2013. Mechanische Rekanalisation bei akutem ischämischen Schlaganfall durch Aspirationsthrombek tomie mit dem Penumbra System: Eine retrospektive Studie, [Mechanical recanalisation in acute ischaemic stroke by aspiration thrombectomy with the Penumbra System - A retrospective study] [INAUGURAL-DISSERTATION]. Göttingen (GER): Universität Göttingen.

Lamprecht S. 2018. In-vitro Untersuchungen zur Interaktion zwischen Thromben und Stentretrievern in Modellen embolisch verschlossener Hirnbasisarterien: [In vitro studies on the interaction between thrombi and stent retrievers in models of embolic occluded basal cerebral arteries] [Dissertation]. Kiel (GER): Christian-Albrechts-Universität.

Leiendecker M-T. 2017. Physikalische Hydrogele auf Polyurethan-Basis: [Physical polyurethane-based hydrogels] [Dissertation]. Potsdam (GER): Universität Potsdam.

Liao Y, Guan M, Liang D, et al. 2020. Differences in pathological composition among large artery occlusion cerebral thrombi, valvular heart disease atrial thrombi and carotid endarterectomy plaques. Front Neurol. 11:811. [accessed 2021 Dec 3]. doi:10.3389/fneur.2020.00811.

Lingenhöhl D. 2017. Ein Gewebe fester als Stahl: [A tissue stronger than steel]. Spektrum.de [Internet]. 2017 Mar 3 [cited 2021 May 6]. https://www.spektrum.de/news/ein-gewebe-fester-als-stahl/1440203.

Liu D, Nikoo M, Boran G, et al. 2015. Collagen and gelatin. Annu Rev Food Sci Technol. 6:527–557. doi:10.1146/annurev-food-031414-111800.

Maekawa K, Shibata M, Nakajima H, et al. 2018. Erythrocyte-Rich Thrombus is associated with reduced number of maneuvers and procedure time in patients with acute ischemic stroke undergoing mechanical thrombectomy. Cerebrovasc Dis Extra. 8:39–49. doi:10.1159/000486042.

Martinod K, Wagner DD. 2014. Thrombosis: tangled up in NETs. Blood. 123:2768–2776. doi:10.1182/blood-2013-10-463646.

McIlvain G, Ganji E, Cooper C, et al. 2019. Reliable preparation of agarose phantoms for use in quantitative magnetic resonance elastography. J Mech Behav Biomed Mater. 97:65–73. doi:10.1016/j.jmbbm.2019.05.001.

Mecke C. 2008. CT-Röntgendichte und MR-Signal von Thromben: [CT radiodensity and MR signal of thrombi] [Dissertation]. Heidelberg, (GER): Universität Heidelberg.

Mfoumou E, Tripette J, Blostein M, et al. 2014. Time-dependent hardening of blood clots quantitatively measured in vivo with shear-wave ultrasound imaging in a rabbit model of venous thrombosis. Thromb Res. 133:265–271. doi:10.1016/j.thromres.2013.11.001.

Mokin M, Setlur Nagesh SV, Ionita CN, et al. 2015. Comparison of modern stroke thrombectomy approaches using an in vitro cerebrovascular occlusion model. AJNR Am J Neuroradiol. 36:547–551. doi:10.3174/ajnr.A4149.

Müller-Esterl W. 2018. Biochemie: Eine Einführung für Mediziner und Naturwissenschaftler [Biochemistry. An introduction for physicians and natural scientists]. 3rd ed. (Lehrbuch). Berlin: Springer Spektrum. doi:10.1007/978-3-662-54851-6.

Nahirnyak VM, Yoon SW, Holland CK. 2006. Acousto-mechanical and thermal properties of clotted blood. J Acoust Soc Am. 119:3766–3772. [accessed 2021 Dec 10]. doi:10.1121/1.2201251.

Nawka MT, Spallek J, Kuhl J, et al. 2020. Evaluation of a modular in vitro neurovascular procedure simulation for intracranial

aneurysm embolization. J Neurointerv Surg. 12:214–219. doi:10.1136/neurintsurg-2019-015073.

Paramasivam S, Baltsavias G, Psatha E, et al. 2014. Silicone models as basic training and research aid in endovascular neurointervention–a single-center experience and review of the literature. Neurosurg Rev. 37:331–337; discussion 337. doi:10.1007/s10143-014-0518-x.

Petrini P, Farè S, Piva A, et al. 2003. Design, synthesis and properties of polyurethane hydrogels for tissue engineering. J Mater Sci Mater Med. 14:683–686. doi:10.1023/a:1024955531173.

Reinhard E, Waeber R, Niederer M, et al. 2001. Preservation of products with MCI/MI in Switzerland. Contact Dermatitis. 45. doi:10.1034/j.1600-0536.2001.450501.x.

Ringleb PA, Hamann GF, Röther J, et al. 2016. Akuttherapie des ischämischen Schlaganfalls – Ergänzung 2015: Rekanalisierende Therapie, [Acute therapy of ischaemic stroke - Supplement 2015. Recanalising therapy]. Leitlinien für Diagnostik und Therapie in der Neurologie, Aufl. 5, 2012. 2016.

Robinson RA, Herbertson LH, Sarkar Das S, et al. 2013. Limitations of using synthetic blood clots for measuring in vitro clot capture efficiency of inferior vena cava filters. Med Devices (Auckl). 6:49–57. [accessed 2021 May 6]. doi:10.2147/MDER.S42555.

Ryan EA, Mockros LF, Weisel JW, et al. 1999. Structural origins of fibrin clot rheology. Biophys J. 77:2813–2826. [cited 2021 Nov 25]. doi:10.1016/S0006-3495(99)77113-4.

Saldívar E, Orje JN, Ruggeri ZM. 2002. Tensile destruction test as an estimation of partial proteolysis in fibrin clots. Am J Hematol. 71:119–127. [accessed 2021 May 6]. doi:10.1002/ajh.10199.

Saver JL. 2006. Time is brain–quantified. Stroke. 37:263–266. [accessed 2021 May 6]. doi:10.1161/01.STR.0000196957.55928.ab.

Saver JL, Goyal M, Bonafe A, et al. 2015. Stent-retriever thrombectomy after intravenous t-PA vs. t-PA alone in stroke. N Engl J Med. 372:2285–2295. doi:10.1056/NEJMoa1415061.

Simon S, Grey CP, Massenzo T, et al. 2014. Exploring the efficacy of cyclic vs static aspiration in a cerebral thrombectomy model: an initial proof of concept study. J Neurointerv Surg. 6:677–683. doi:10.1136/neurintsurg-2013-010941.

Slaboch CL, Alber MS, Rosen ED, et al. 2012. Mechano-rheological properties of the murine thrombus determined via nanoindentation and finite element modeling. J Mech Behav Biomed Mater. 10:75–86. doi:10.1016/j.jmbbm.2012.02.012.

Spallek J, Kuhl J, Wortmann N, et al.. 2019. Design for mass adaptation of the neurointerventional training model HANNES with patient-specific aneurysm models. In: Proceedings of the Design Society: International Conference on Engineering Design; p. 897–906.

Staessens S, Denorme F, Francois O, et al. 2020. Structural analysis of ischemic stroke thrombi: histological indications for therapy resistance. Haematologica. 105:498–507. doi:10.3324/haematol.2019.219881.

Teng Z, Feng J, Zhang Y, et al. 2015. Layer- and direction-specific material properties, extreme extensibility and ultimate material strength of human abdominal aorta and aneurysm: a uniaxial extension study. Ann Biomed Eng. 43:2745–2759. doi:10.1007/s10439-015-1323-6.

Verein Deutscher Ingenieure e.V. 2019. Design of technical products and systems Configuration of individual product design processes. November 2019 [cited 2021 Feb 10]. Düsseldorf (GER): VDI-Handbuch Produktentwicklung und Konstruktion. (vol. 03.100.40).

Vidmar J, Serša I, Kralj E, et al. 2015. Unsuccessful percutaneous mechanical thrombectomy in fibrin-rich high-risk pulmonary thromboembolism. Thromb J. 13:30. doi:10.1186/s12959-015-0060-2.

Vitello DJ, Ripper RM, Fettiplace MR, et al. Blood density is nearly equal to water density: a validation study of the gravimetric method of measuring intraoperative blood loss. J Vet Med. 2015;2015. [cited 2021 Dec 10]. doi:10.1155/2015/152730.

Vock P, Woermann U. 2021. RadioSurf: Prinzip der Strahlenschwächung: [RadioSurf: Principle of beam attenuation] [Internet] [cited 2021 May 6]. https://radiosurf.elearning.aum.iml.unibe.ch/htmls/slide.html?radiosurf% 7Cradskull lct% 7Cbasics% 7Ctechnic% 7C1#.

Walker BS, Shah LM, Osborn AG. 2014. Calcified cerebral emboli, a “do not miss” imaging diagnosis: 22 new cases and review of the literature. AJNR Am J Neuroradiol. 35:1515–1519. doi:10.3174/ajnr.A3892.

Wang DH, Makaroun M, Webster MW, et al. 2001. Mechanical properties and microstructure of intraluminal thrombus from abdominal aortic aneurysm. J Biomech Eng. 123:536–539. doi:10.1115/1.1411971.

Weafer FM, Duffy S, Machado I, et al. 2019. Characterization of strut indentation during mechanical thrombectomy in acute ischemic stroke clot analogs. J Neurointerv Surg. 11:891–897. doi:10.1136/neurintsurg-2018-014601.

Wetzel SG, Ohta M, Handa A, et al. 2005. From patient to model: stereolithographic modeling of the cerebral vasculature based on rotational angiography. AJNR Am J Neuroradiol [Internet]. 26:1425–1427. http://www.ajnr.org/content/26/6/1425.

Wortmann N, Krause D, Fiehler J, et al. 2021. inventor;, assignee. Synthetisches Thrombusmodell zum Erlernen der operativen Entfernung eines Blutgerinnsels im Rahmen einer Behandlungsnachstellung, [Synthetic thrombus model for learning the surgical removal of a blood clot in the context of a treatment readjustment]. patented pending.

Xie H, Kim K, Aglyamov SR, et al. 2005. Correspondence of ultrasound elasticity imaging to direct mechanical measurement in aging DVT in rats. Ultrasound Med Biol. 31:1351–1359. doi:10.1016/j.ultrasmedbio.2005.06.005.

Yuki I, Kan I, Vinters HV, et al. 2012. The impact of thromboemboli histology on the performance of a mechanical thrombectomy device. AJNR Am J Neuroradiol. 33:643–648. doi:10.3174/ajnr.A2842.